RESEARCH/REVIEW ARTICLE

# Biogenic and detrital-rich intervals in central Arctic Ocean cores identified using x-ray fluorescence scanning

Daniela Hanslik,[1] Ludvig Löwemark[2,3] & Martin Jakobsson[1]

[1] Department of Geological Sciences, Stockholm University, SE-106 91 Stockholm, Sweden
[2] Department of Geosciences, National Taiwan University, No. 1, Sec. 4, Roosevelt Road, 106 Taipei, Taiwan
[3] Climate Science Division, Alfred Wegener Institute for Polar and Marine Research, Bussestraße 24, DE-27570, Bremerhaven, Germany

**Keywords**
Foraminifera; Arctic Ocean; IRD; calcareous microfossils; XRF scanning.

**Correspondence**
Ludvig Löwemark, Department of Geosciences, National Taiwan University, No. 1, Sec. 4, Roosevelt Road, 106 Taipei, Taiwan. Email: loewemark@gmail.com

## Abstract

X-ray fluorescence (XRF) scanning of sediment cores from the Lomonosov Ridge and the Morris Jesup Rise reveals a distinct pattern of Ca intensity peaks through Marine Isotope Stages (MIS) 1 to 7. Downcore of MIS 7, the Ca signal is more irregular and near the detection limit. Virtually all major peaks in Ca coincide with a high abundance of calcareous microfossils; this is particularly conspicuous in the cores from the central Arctic Ocean. However, the recorded Ca signal is generally caused by a combination of biogenic and detrital carbonate, and in areas influenced by input from the Canadian Arctic, detrital carbonates may effectively mask the foraminiferal carbonates. Despite this, there is a strong correlation between XRF-detected Ca content and foraminiferal abundance. We propose that in the Arctic Ocean north of Greenland a common palaeoceanographic mechanism is controlling Ca-rich ice-rafted debris (IRD) and foraminiferal abundance. Previous studies have shown that glacial periods are characterized by foraminfer-barren sediments. This implies that the Ca-rich IRD intervals with abundant foraminifera were most likely deposited during interglacial periods when glaciers left in the Canadian Arctic Archipelago were still active and delivered a large amount of icebergs. At the same time, conditions were favourable for planktic foraminifera, resulting in a strong covariance between these proxies. Therefore, we suggest that the XRF scanner's capability to efficiently map Ca concentrations in sediment cores makes it possible to systematically examine large numbers of cores from different regions to investigate the palaeoceanographic reasons for the calcareous microfossils' spatial and temporal variability.

The Quaternary sediment record in central Arctic Ocean cores is characterized by discontinuous preservation of calcareous micro- and nannofossil fauna and flora and dark brown, more or less bioturbated, intervals enriched in manganese (Jakobsson et al. 2000; Löwemark et al. 2008; Adler et al. 2009; Sellén et al. 2010; Löwemark et al. 2012). Beyond the radiocarbon dating limit of 40–50 Ky, the age models of these cores have primarily been based on a variety of relative dating methods (Backman et al. 2004). One of the most commonly used methods to establish age models is to correlate the downcore variations of stable oxygen isotopes, measured on benthic foraminifera, to a stacked global deep-ocean record (Lisiecki & Raymo 2005). However, this approach is of limited use in the Arctic Ocean because of the discontinuous occurrence of calcareous foraminifera in combination with large influences of varying freshwater influx over time (e.g., Stein et al. 1994; Spielhagen et al. 2004). Instead, cycles of dark brown, manganese-rich layers have been correlated to the global deep-ocean oxygen isotope record because the cycles are interpreted to represent glacial–interglacial palaeoceanographic variations, where the dark brown units represent warmer periods with enhanced Mn input from Siberian rivers


Citation: *Polar Research* 2013, *32*, 18386, http://dx.doi.org/10.3402/polar.v32i0.18386

and coastal erosion on the Siberian shelves (Jakobsson et al. 2000; Löwemark et al. 2008; März et al. 2011; Macdonald & Gobeil 2012). To constrain the cyclicity in time, some benthic foraminifera as well as calcareous nannofossils are used as biostratigraphic markers. For example, Marine Isotope Stage (MIS) 5.5 has been identified in central Arctic Ocean cores by the presence of the calcareous nannofossil *Emiliania huxleyi* (Gard 1993; Backman et al. 2004; Backman et al. 2009). However, only the cycles younger than MIS 6 contain abundant and well preserved calcareous microfossils. Below MIS 6 planktic foraminifera occur in some cores during MIS 7 (Jakobsson et al. 2000; Backman et al. 2004; O'Regan et al. 2008), but are seldom found below MIS 7. Calcareous benthic foraminifera are typically replaced by an agglutinated assemblage during MIS 7–9 (Cronin et al. 2008).

The palaeoceanographic reason(s) for the spatial and temporal discontinuity in the occurrence of calcareous micro- and nannofossils is not known. For example, the spatial discontinuity is exemplified by studies of cores acquired from the Lomonosov Ridge (Fig. 1) during the Arctic Coring Expedition (ACEX), part of the Integrated Ocean Drilling Program Expedition 302 (Backman et al. 2006), and core HLY0503-18TC from the Healy–Oden Trans-Arctic Expedition of 2005 (HOTRAX; Darby et al. 2009). These cores do not contain calcareous microfossils in the sediment unit associated with MIS 5.5 (O'Regan et al. 2008; Backman et al. 2009; Hanslik et al. 2010). In contrast, cores less than 100 km away from the ACEX sites on the Lomonosov Ridge (cores 96/12-1pc and PS2185; Fig. 1), in similar water depths of about 1000 m, contain abundant calcareous micro- and nannofossils in the MIS 5.5 unit (Jakobsson et al. 2000; Spielhagen et al. 2004).

To further address the cause of spatial and temporal differences regarding calcareous microfossil occurrence in central Arctic Ocean cores, it would be necessary to investigate large numbers of cores from different water depths and a variety of regions. However, analyses of microfossil content are time consuming, often requiring a large amount of material, and therefore, the common praxis is to concentrate micropalaeontologic studies to selected key cores.

X-ray fluorescence (XRF) core scanning, on the other hand, is a fast, non-destructive method that provides a continuous profile of relative variations in major and trace elements in sediment cores. For example, the manganese enriched sediment cycles were readily identified with the Itrax XRF scanner (Löwemark et al. 2008). In this study, we demonstrate that the cores retrieved during the Lomonosov Ridge off Greenland Expedition (LOMROG) of 2007 with the ice-breaker *Oden* (Jakobsson, Marcussen et al. 2008) can be correlated using Ca concentration variations measured with the Itrax XRF core scanner. We also show that the highest abundance of calcareous microfossils in the sediment cores from the southern Lomonosov Ridge off Greenland and the Morris Jesup Rise coincide with elevated XRF Ca-intensity intervals, providing strategic sub-sampling guidance. Furthermore, the studied LOMROG cores contain planktic and benthic foraminifera at deeper core depth than previously found in central Arctic Ocean cores, suggesting better calcareous preservation at this Arctic Ocean exit gateway to the North Atlantic. Thus, by placing our new results in the greater context of spatial and temporal variations in Arctic sedimentary Ca and carbonate variations, a better understanding of the underlying mechanisms can be obtained.

## Material and methods

Six cores retrieved during the LOMROG expedition from the southern Lomonosov Ridge north of Greenland and the Morris Jesup Rise are included in this study (Table 1; Fig. 1). The full names of these cores include the prefix LOMROG07, which hereafter is omitted. Two of the LOMROG cores were analysed for planktic and benthic foraminifera: core PC-04 with a total length of 5.3 m retrieved from the southern Lomonosov Ridge crest at 811 m water depth, and PC-08 with a total length of 5.9 m retrieved from the shallow crest of the Morris Jesup Rise at 1038 m water depth (Fig. 1). Subsamples of approximately 5 cc were taken every fourth centimetre from core PC-04 and every fifth centimetre from core PC-08. They were freeze-dried and wet-sieved with a 63 μm sieve for grain size analysis. Thereafter, the samples were dry-sieved using a 125 μm sieve for the microfossil analyses. Both planktic and benthic foraminifera were identified at the species level. However, in this study only the numbers of foraminifera per gram sediment and the benthic species used as chronostratigraphic markers are presented.

The working halves of the LOMROG cores (GC-02, PC-04, PC-06, PC-07, PC-08 and GC-10) were measured with the Itrax XRF core scanner at Stockholm University core processing laboratory. A detailed description of the Itrax core scanner is provided by Croudace et al. (2006). Measurements were carried out using a molybdenum tube operated at 30 kV and 25 mA with a sampling resolution of 0.1 cm and a 4 s exposure time (PC-06, PC-08, GC-10) or 0.5 cm resolution and 20 s exposure time (GC-02, PC-04, PC-07) with data output in counts rather than element concentration. The Ca counts were normalized by the sum of incoherent and coherent scattering (see, e.g., Löwemark et al. 2011; Kylander et al. 2012) to


Citation: *Polar Research* 2013, *32*, 18386, http://dx.doi.org/10.3402/polar.v32i0.18386

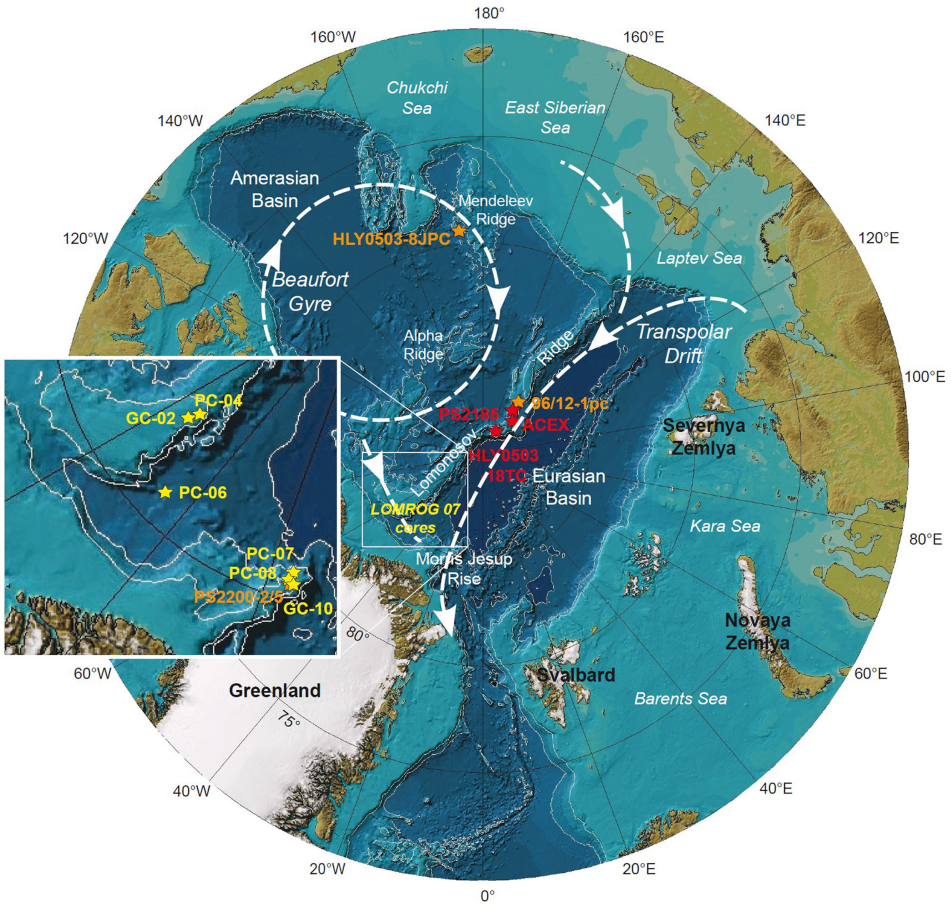


**Fig. 1** Map of the Arctic Ocean (Jakobsson, Macnab et al. 2008) with an inset showing the position of the cores from the 2007 Lomonosov Ridge off Greenland Expedition (LOMROG) in yellow, core PS2200-2/5 from the Morris Jesup Rise, core 96/12-1pc from the Lomonosov Ridge and core HLY0503-8JPC from the Mendeleev Ridge (orange). Also indicted are key cores from the Lomonosov Ridge, Arctic Coring Expedition (ACEX) and PS2185 and a core from the Lomonosov Ridge Intra Basin, HLY0503-18TC (red). White arrows indicate surface water and ice circulation pattern of the Transpolar Drift and the Beaufort Gyre.

remove various effects of the sample matrix, as water content and density, and detector dead times. The data have been smoothed and plotted with a running mean over 3 cm (Fig. 2). Ca measurement data can be downloaded from the Bert Bolin Centre for Climate Research database (www.bbcc.su.se).

The age model for core PC-08 was adopted from the nearby core PS2200-2/5 (Nørgaard-Pedersen et al. 1998; Spielhagen et al. 2004) with slight modifications taking the benthic foraminifera results into account (Fig. 3). The age model for core 96/12 is described in Jakobsson et al. (2000) and cores GC-02 and GC-10 are correlated to core

**Table 1** Core locations for 2007 Lomonosov Ridge off Greenland Expedition cores and other cited cores.

| Core | Latitude | Longitude | Water depth | Core length |
|---|---|---|---|---|
| GC-02 | N 86°37.91' | W 054°09.07' | 723 m | 223 cm |
| PC-04 | N 86°42.07' | W 053°46.03' | 811 m | 523 cm |
| PC-06 | N 85°29.60' | W 046°16.40' | 3009 m | 400 cm |
| PC-07 | N 85°23.98' | W 014°16.92' | 1252 m | 463 cm |
| PC-08 | N 85°19.19' | W 014°51.45' | 1038 m | 592 cm |
| GC-10 | N 85°17.59' | W 014°48.88' | 1017 m | 247 cm |
| 96/12 | N 87°05.9' | E 144°46.4' | 1003 m | 722 cm |
| 8JPC | N 79°35.6' | W 172°30.1' | 2792 m | 1188 cm |
| PS2200 | N 85°19.6' | W 014°01.3' | 1073 m | 725 cm |

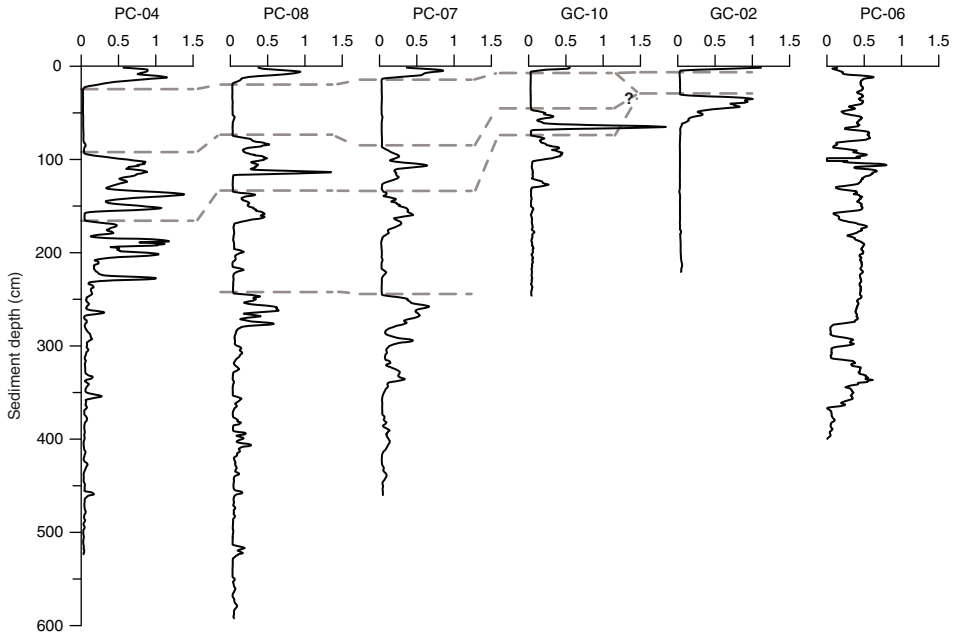


**Fig. 2** Correlation of the selected 2007 Lomonosov Ridge off Greenland Expedition cores based on Ca intensity variations. Ca data have been normalized by incoherent and coherent scattering.

96/12 using the nannofossil stratigraphy presented in Jakobsson et al. (2010).

To test whether our identification of calcareous foraminiferal abundance using XRF Ca records can be extended to other parts of the Arctic Ocean, previously studied cores from the central Lomonosov Ridge, Mendeleev Ridge and the Morris Jesup Rise are included (Table 1; Figs. 1, 4). Core 96/12-1pc (hereafter referred to as core 96/12) from the crest of the central Lomonosov Ridge (1003 m water depth) was scanned continuously over 0.5 cm intervals with an exposure time of 10 s (Löwemark et al. 2008). These measured variations in Ca are compared with the previously obtained foraminiferal record of this core published by Jakobsson et al. (2001). Core HLY0503-8JPC (hereafter referred to as core 8JPC) from the Mendeleev Ridge (2792 m water depth) was measured using an energy-dispersive Alpha series handheld XRF analyser (Innov-X, Woburn, MA, USA) at increments between 2 and 6 cm with detection limits in the range of 10–100 ppm (Polyak et al. 2009). The foraminiferal record of core 8JPC has been published by Adler et al. (2009). Core PS2200-2/5 from the Morris Jesup Rise (1073 m water depth) was analysed by Vogt (1997) for calcium carbonate and dolomite by x-ray diffraction (XRD) each fifth centimetre and the foraminiferal record was published by Spielhagen et al. (2004). The data set for core PS2200-2/5 can also be found at www.pangaea.de

## Results

### Foraminifera

The planktic foraminiferal abundances of the >125 μm size fraction in cores PC-04 and PC-08 show four major intervals containing >2000 specimens per gram dry sediment (Fig. 3). The upper three of these peaks seem to correlate with each other, while the fourth peaks likely represent different events in the two cores. The planktic foraminiferal peak at around 300 cm in core PC-04 is composed of *Turborotalita quinqueloba*. This composition is different compared to the other peaks in both cores since they are to about 95% composed of *Neogloboquadrina pachyderma* sinistral. Below 300 cm in core PC-08 and 320 cm in core PC-04 planktic foraminifera occur only sporadically and in low numbers.

Peaks of benthic foraminiferal abundances are found in the upper 300 cm of both cores at the same intervals as the planktic, with the exception of an additional benthic peak around 250 cm in core PC-04 (Fig. 3a). The maximum number of benthic foraminifera in the upper 300 cm of core PC-04 approaches 3000 individuals per gram dry sediment at 240 cm, and the average for the studied samples containing at least one foraminifer is about 400. In core PC-08, the maximum abundance is found at about 95 cm, where 1000 specimens per gram dry sediment are found, and the average for the core is approximately 230. Below 300 cm, where there are no major planktic


Citation: *Polar Research* 2013, *32*, 18386, http://dx.doi.org/10.3402/polar.v32i0.18386

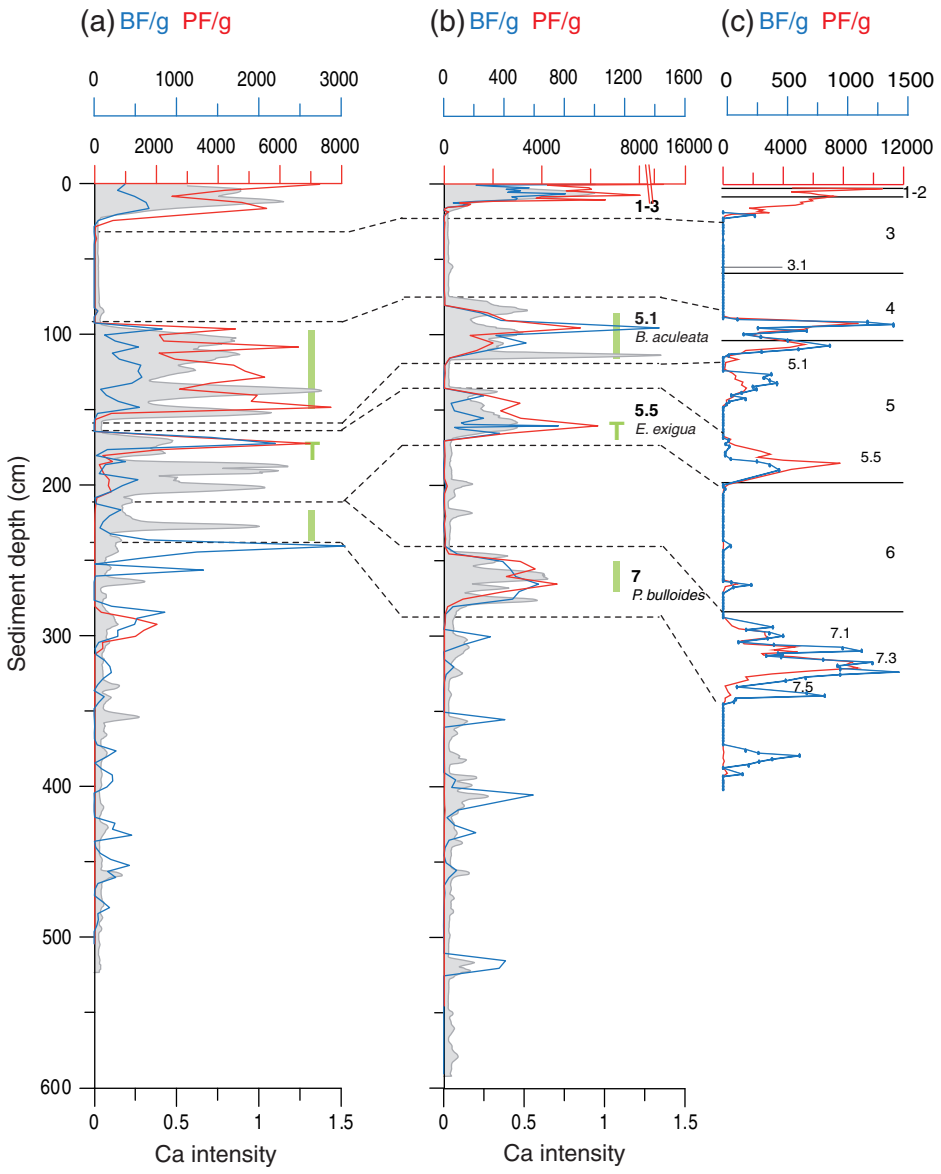


**Fig. 3** Correlation between core (a) PC-04, (b) PC-08 and (c) PS2200-2/5 with the planktic foraminiferal abundances per gram dry sediment (PF/g, shown with a red line), benthic foraminiferal abundance per gram (BF/g, shown with a blue line) and Ca counts normalized by incoherent and coherent scattering as the shaded grey areas. Chronology for core PS2200-2/5 as published by Spielhagen et al. (2004) is given through Marine Isotope Stages (MIS) 1–7 and the correlated stages for cores PC-04 and PC-08 are indicated in PC-08. Benthic time marker events for *Bulimina aculeata* and *Pullenia bulloides* are indicated by green bars and the last appearance of *Epistominella exigua* by a green ''T'' for core PC-04 and the corresponding interval in core PC-08.

abundance peaks in any of the two cores, benthic foraminifera occur in both cores with several prominent peaks. The average specimen abundance is lower; about 95 specimens per gram sediment in core PC-04 and about 85 specimens in core PC-08. Furthermore, the percentage of agglutinated benthic species increases to comprise of up to 15% of all the species. However, we do not find a complete switch to an exclusive agglutinated fauna, which have been described in studies of several other central Arctic Ocean cores (Cronin et al. 2008).

Intervals of commonly used benthic chronostratigraphic markers are shown in Fig. 3. These were used to establish the age models of cores PC-04 and PC-08 and to correlate the cores with each other. The inferred age models are further described below. The age indicative species are *Bulimina aculeata* for MIS 5.1 (Jakobsson et al. 2001; Backman et al. 2004), the last appearance of *Epistominella exigua* in MIS 5.5 (Hanslik 2011) and *Pullenia bulloides* for MIS 7 (Jakobsson et al. 2001; Backman et al. 2004). A description of the planktic and

benthic foraminiferal assemblage and abundance of core 96/12 (Fig. 4a) is found in Jakobsson et al. (2001). Figure 4 also shows the planktic foraminifera record of core 8JPC from Adler et al. (2009) and the planktic record and grain size distribution of core PS2200-2/5 from Spielhagen et al. (2004).

## Itrax XRF

Among all the chemical elements measured by XRF scanning in cores PC-04 and PC-08, Ca stands out as it displays a distinct and almost cyclic pattern in the upper part of the cores (Figs. 2, 3). Four distinct intervals of higher relative Ca intensity occur in the upper 300 cm of core PC-08, while a number of low-amplitude peaks are found in the lower part of the core (Fig. 3b). The pattern in core PC-04 is less distinct, but still three intervals with higher Ca counts can be distinguished in the upper 250 cm from lower values further down core (Fig. 3a). The peak Ca intervals are on average higher and more frequent in core PC-04 compared to PC-08, which is most likely linked to their geographical position in the Arctic Ocean and the surface water circulation with a stronger influence of material transported by the Beaufort Gyre to the southern Lomonosov Ridge. Core PC-07, located on the Morris Jesup Rise, shows a similar pattern to that of close-by core PC-08. However, the shorter gravity core GC-10 retrieved from an iceberg scoured area on the Morris Jesup Rise (Jakobsson et al. 2010) shows a deviant pattern below 120 cm caused by sever iceberg erosion removing large quantities of sediment. Other signs of disturbance can be identified in core GC-02, from 723 m water depth on the Lomonosov Ridge, and especially in core PC-06 from the south-east spur of the Lomonosov Ridge at 3009 m water depth (Fig. 2). In core 96/12 two intervals with elevated Ca concentration are clearly seen, the first in the top 15 cm of the core and the second between 160 and 230 cm (Fig. 4a).

The intervals in cores PC-04 and PC-08 with elevated Ca counts are associated with increased calcareous foraminiferal abundance (Fig. 3a, b). Highest foraminiferal abundances are reached in conjunction with major Ca peaks. However, a more detailed inspection of core PC-08 reveals that some parts of the interval with higher Ca ratios between about 75 and 115 cm, as well as the highest peak centred at 115 cm, cannot be matched with foraminiferal abundance (Fig. 3b). A comparison with the visual core description of PC-08 shows that the 115 cm peak is due to a light coloured detrital carbonate layer. Unfortunately, because Mg is outside the detectable range for the Itrax XRF scanner, a distinction of biogenic from detrital carbonates using a comparison between Mg/Al and Ca/Al ratios as suggested by März et al. (2011) could not be made. Further downcore, the elevated Ca counts generally correspond with enhanced foraminifer abundance, although several smaller Ca-peaks without the corresponding increase in foraminifers were observed.

A similar pattern of agreement between XRF Ca intensity and foraminiferal abundance is found in core 96/12 in the upper part of the core, where calcareous foraminifera are present (Fig. 4a).

## Age model and correlation

The chronology for cores PC-04 and PC-08 was obtained through correlation to core PS2200-2/5 (Fig. 3; Table 2) for which the age model was initially established using radiocarbon dating and correlation to core PS2185 on the Lomonosov Ridge using, amongst other approaches, palaeomagnetism, coarse grain fraction and mineralogy (Vogt 1997; Spielhagen et al. 2004). In turn, PS2185 is correlated to core AO96/12-1pc where the age model, in addition to first being established using nannofossil biostratigraphy, palaeomagnetism and manganese cyclostratigraphy, has been constrained using optically stimulated luminescence dating (Jakobsson et al. 2003). The prominent four upper peaks in foraminiferal abundance show a nearly identical pattern in cores PC-08 and PS2200-2/5 (Fig. 3b, c). However, we suggest one change in PS2200's age model since *B. aculeata,* a key chronostratigraphic marker first occurring in late MIS 5 (Backman et al. 2004), is found in the interval between 85 and 115 cm in core PC-08 (Fig. 3b). The previous PS2200 age model assigned the corresponding peak to MIS 4 (Spielhagen et al. 2004). Further, the last occurrence of *E. exigua* at 155 cm in PC-08 was used as a time marker for early MIS 5 and *P. bulloides* occurrence between 250 and 270 cm for MIS 7 (Jakobsson et al. 2001; Backman et al. 2004). The planktic and benthic foraminiferal peaks in association with benthic chronostratigraphic markers and Ca XRF pattern were used for correlation between cores PC-08 and PC-04.

## Discussion and conclusion

The Itrax XRF results from the investigated cores display an unambiguous correspondence between foraminiferal abundance and Ca signal in the time interval from MIS 7 to the present. Below MIS 7, however, the Ca signal is less clear with more frequent lower intensity peaks in the sediments, and planktic foraminifera are generally few or absent. This general disappearance of calcium carbonate below MIS 7 is characteristic for central Arctic Ocean


Citation: *Polar Research* 2013, *32*, 18386, http://dx.doi.org/10.3402/polar.v32i0.18386

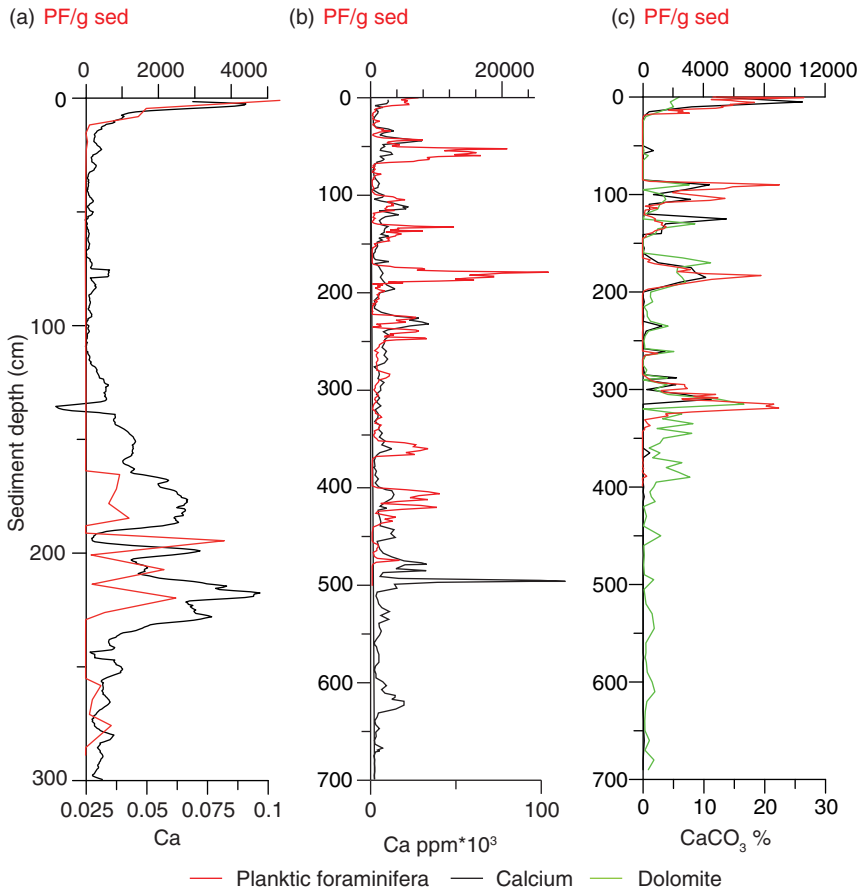


**Fig. 4** Other central Arctic Ocean cores from (a) Lomonosov Ridge (96/12), (b) Mendeleev Ridge (8JPC; Adler et al. 2009) and (c) the Morris Jesup Rise (PS2200-2/5; Spielhagen et al. 2004) show a strong general connection between foraminiferal abundance (red line) and Ca (black line).

cores (Backman et al. 2004) and is further corroborated by measurements of discrete samples in core PS2200-2/5 from the Morris Jesup Rise (Vogt 1997). Exceptions to this pattern are found in several parts of the Arctic Ocean where calcareous microfossils are absent from below MIS 5 or even, in some cases, from below MIS 3 (Hanslik et al. 2010). In LOMROG cores PC-04 and PC-08 calcareous benthic foraminifera are, in contrast, still present below MIS 7, and peaks in abundance correspond to smaller maxima in Ca.

**Table 2** Age model for the studied cores PC-04 and PC-08.

| Depth (cm) | Marine Isotope Stage | Age (thousands of years) |
|---|---|---|
| PC-04 | | |
| 0–40 cm | MIS 1–3 | 0–60 |
| 90–150 cm | MIS 5.1 | 85 |
| 170–210 cm | MIS 5.5 | 130 |
| 215–230 cm | MIS 7 | 244 |
| PC-08 | | |
| 0–20 cm | MIS 1–3 | 0–60 |
| 75–120 cm | MIS 5.1 | 85 |
| 135–170 cm | MIS 5.5 | 130 |
| 240–290 cm | MIS 7 | 244 |

There is a highly uneven spatial distribution of detrital carbonate and dolomite in central Arctic Ocean surface sediments. Concentrations measured by XRD in the bulk sediments of the Eurasian Basin are low (0–3%) but can reach values of up to 27% on the Morris Jesup Rise (Vogt 1997). High abundance of clasts of dolostone/limestone is also observed throughout the Amerasian Basin (Phillips & Grantz 2001). This distribution pattern is the result of transport of carbonate and dolomite from their main source areas in the Canadian Arctic via the surface water and sea-ice circulation system, which is dominated by the Beaufort Gyre in the Amerasian Basin (Fig. 1). Little of this material contributes to the sediments of the Eurasian Basin, where the Transpolar Drift primarily dictates the surface circulation regime.

The highest Ca peaks are seen in detrital carbonate layers commonly visible as a white layer in the lithology. This is seen, for example, around 115 cm in core PC-08. Similar layers are observed in cores throughout the

Amerasian Basin (Clark et al. 1980; Phillips & Grantz 2001; Polyak et al. 2004) and described as "pinkish-white layers" with carbonate contents of >30% (Clark et al. 1980). Most carbonate clasts have their main source area in Palaeozoic carbonates from Alaska, north-western Canada and the Canadian Arctic Archipelago (Bischof 2000). It has been suggested that they have been transported into the Arctic Basin by icebergs calved from the Laurentide Ice Sheet, especially in the beginning of glacial and interglacial cycles during the more active ice-sheet build-up or decay periods (Phillips & Grantz 2001). The ice-rafted debris, including detrital carbonate, is released along the ice drift path across the Amerasian Basin and further over the southern Lomonosov Ridge off northern Greenland and the Morris Jesup Rise before exiting the Arctic through the Fram Strait. An additional minor source of non-biogenic carbonates can be found in Northwestern Greenland contributing to the sediments found at the Morris Jesup Rise (Vogt 1997).

A valid question is how much of the Ca signal measured with the Itrax XRF is due to detrital carbonates and how much is due to biogenic input of calcareous microfossils? Detrital Ca base levels in the central Arctic typically range from 1% to 2% (Al-Hanbali 2000). As peak foraminiferal content in the sediment may reach well over 5000 tests/g (Figs. 3, 4) and individual test weights range 1–16 μg (with typical values around 6 μg; Stangeew 2001), the carbonate content contributed by foraminifera may reach 3% or more (5000 tests * 6 μg/test = 30 000 μg/g = 3% carbonate = 1.2% Ca). Consequently, foraminiferal abundance can play a role in controlling the Ca signal detected by the Itrax XRF scanner in areas with low background input of terrigenous Ca, such as the central Lomonosov Ridge (Fig. 4a) and parts of the Eurasian Basin (Vogt 1997).

The cores from the southern Lomonosov Ridge and the Morris Jesup Rise are, however, characterized by peak intervals with much more than a few percent Ca. This is shown by the XRD measurements, which yield Ca contents up to 10–20% (Fig. 4c). Such highs are not only composed of calcite and dolomite clasts as Ca may reside also in the silt and clay size fraction (Vogt 1997). Therefore, we conclude that only a minor amount of the measured Ca intensity in cores PC-04 and PC-08 is contributed by foraminifera and the major part is the result of detrital carbonate input. However, foraminiferal abundances and Ca intensity measurements display a strong correlation and almost no foraminifera are found in intervals with low Ca content. The Holocene oceanographic conditions in the central Arctic Ocean permit preservation of calcareous microfossils, and this also appears to have been the case for previous interglacials. During interglacial times, when sea-ice conditions are favourable for foraminifera, the remaining largest active glaciers in the circumarctic region are found on Greenland and in the Canadian Arctic. These are two areas characterized by large regions of carbonate bedrock from which detrital components eroded by glaciers can be spread over the Arctic Ocean through the surface circulation, particularly by the Beaufort Gyre as described above (Bischof 2000). At present, extensive biological production takes place during summers over the wide Arctic Ocean shelves (Anderson et al. 2010). The decay products, nutrients and dissolved inorganic carbon from the shelves are drawn down to deeper depths of the central basin with the waters produced along the shelves during sea-ice formation. This process creates heavier waters with relatively low pH and a low degree of calcium carbonate saturation (Anderson et al. 2010), but the acidity is obviously not enough—under present conditions—to prevent calcium carbonate shells of foraminifera from reaching the seafloor and accumulating in the surface sediments. During glacial conditions severe sea-ice conditions most likely reduced foraminifer production to an absolute minimum. Therefore, the explanation for the glacial—interglacial swings in foraminifer abundance is rather straightforward. In contrast, the large spatial variability in foraminifer abundance during interglacial intervals still remains elusive. Only a comprehensive study of sediment cores from different regions and depths will produce a testable hypothesis to account for this variability. In this context, Itrax scanning would provide a valuable non-destructive first analysis of the sediment cores. It still remains unclear why calcareous benthic foraminifera can be observed in intervals in the lower part of the investigated cores, whereas planktic foraminifera are basically absent. To understand the palaeoceanographic conditions responsible for the spatial differences in the occurrence of calcareous microfossil in Arctic Ocean Pleistocene sediments, more cores will have to be investigated systematically, both from different regions and depths. Despite the limitations in the XRF scanner technique, such as reporting counts rather than absolute concentrations, and not allowing comparisons of absolute values between different cores because of differences in water content, grain size and x-ray tube aging (Tjallingii et al. 2007; Weltje & Tjallingii 2008), the XRF data comprise a powerful correlation tool, a reliable first proxy for foraminiferal abundance variation and a useful guide for targeted subsampling.



Citation: *Polar Research* 2013, *32*, 18386, http://dx.doi.org/10.3402/polar.v32i0.18386

## Acknowledgements

This is a contribution from the Bert Bolin Centre for Climate Research. Reviews by T. Richter and G. Kuhn helped to improve the manuscript.

## References

Adler R.E., Polyak L., Ortiz J.D., Kaufman D.S., Channell J.E.T., Xuan C., Grottoli A.G., Sellen E. & Crawford K.A. 2009. Sediment record from the western Arctic Ocean with an improved Late Quaternary age resolution: HOTRAX core HLY0503-8JPC, Mendeleev Ridge. *Global and Planetary Change 68*, 18–29.

Al-Hanbali H. 2000. *The geochemistry of two selected areas of the deep sea: the TAG hydrothermal mound, Mid-Atlantic Ridge and the Lomonosov Ridge, central Arctic Ocean*. Stockholm: Stockholm University.

Anderson L.G., Tanhua T., Bjork G., Hjalmarsson S., Jones E.P., Jutterstrom S., Rudels B., Swift J.H. & Wahlstom I. 2010. Arctic ocean shelf–basin interaction: an active continental shelf $CO_2$ pump and its impact on the degree of calcium carbonate solubility. *Deep-Sea Research Part I 57*, 869–879.

Backman J., Fornaciari E. & Rio D. 2009. Biochronology and paleoceanography of late Pleistocene and Holocene calcareous nannofossil abundances across the Arctic Basin. *Marine Micropaleontology 72*, 86–98.

Backman J., Jakobsson M., Lovlie R., Polyak L. & Febo L.A. 2004. Is the central Arctic Ocean a sediment starved basin? *Quaternary Science Reviews 23*, 1435–1454.

Backman J., Moran K., McInroy D.B., Mayer L.A. & the Expedition 302 Scientists 2006. *Proceedings of the Integrated Ocean Drilling Program. Vol. 302*. Edinburgh: Integrated Ocean Drilling Program Management International.

Bischof J. 2000. *Ice drift, ocean circulation and climate change*. Chichester, UK: Springer.

Clark D.L., Whitman R.R., Morgan K.A. & Mackey S.D. 1980. *Stratigraphy and glacial–marine sediments of the Amerasian Basin, central Arctic Ocean. Geological Society of America Special Paper 181*. Boulder: Geological Society of America.

Cronin T.M., Smith S.A., Eynaud F., O'Regan M. & King J. 2008. Quaternary paleoceanography of the central Arctic based on Integrated Ocean Drilling Program Arctic Coring Expedition 302 foraminiferal assemblages. *Paleoceanography 23*, PA1S18, doi: 10.1029/2007PA001484.

Croudace I.W., Rindby A. & Rothwell R.G. 2006. ITRAX: description and evaluation of a new multi-function x-ray core scanner. In: R.G. Rothwell (ed.): *New techniques in sediment core analysis*. Pp. 51–63. London: Geological Society of London.

Darby D.A., Polyak L. & Jakobsson M. 2009. The 2005 HOTRAX expedition to the Arctic Ocean. *Global and Planetary Change 68*, 1–4.

Gard G. 1993. Late Quaternary coccoliths at the North Pole: evidence of ice-free conditions and rapid sedimentation in the central Arctic Ocean. *Geology 21*, 227–330.

Hanslik D. 2011. *Late Quaternary biostratigraphy and paleoceanography of the central Arctic Ocean*. PhD thesis, Stockholm University, Stockholm, 32 pp.

Hanslik D., Jakobsson M., Backman J., Björck S., Sellén E., O'Regan M., Fornaciari E. & Skog G. 2010. Quaternary Arctic Ocean sea ice variations and radiocarbon reservoir age corrections. *Quaternary Science Reviews 29*, 3430–3441.

Jakobsson M., Lovlie R., Al-Hanbali H., Arnold E., Backman J. & Morth M. 2000. Manganese and color cycles in Arctic Ocean sediments constrain Pleistocene chronology. *Geology 28*, 23–26.

Jakobsson M., Lovlie R., Arnold E.M., Backman J., Polyak L., Knutsen J.O. & Musatov E. 2001. Pleistocene stratigraphy and paleoenvironmental variation from Lomonosov Ridge sediments, central Arctic Ocean. *Global and Planetary Change 31*, 1–22.

Jakobsson M., Macnab R., Mayer L., Anderson R., Edwards M., Hatzky J., Schenke H.W. & Johnson P. 2008. An improved bathymetric portrayal of the Arctic Ocean: implications for ocean modeling and geological, geophysical and oceanographic analyses. *Geophysical Research Letters 35*, L07602, doi: 10.1029/2008GL033520.

Jakobsson M., Marcussen C. & LOMROG Scientific Party 2008. *Lomonosov Ridge off Greenland 2007 (LOMROG). Cruise report*. Copenhagen: Geological Survey of Denmark and Greenland.

Jakobsson M., Nilsson J., O'Regan M., Backman J., Löwemark L., Dowdeswell J.A., Mayer L., Polyak L., Colleoni F., Anderson L.G., Björk G., Darby D., Eriksson B., Hanslik D., Hell B., Marcussen C., Sellen E. & Wallin Å. 2010. An Arctic Ocean ice shelf during MIS 6 constrained by new geophysical and geological data. *Quaternary Science Reviews 29*, 3505–3517.

Kylander M.E., Lind E.M., Wastegård S. & Löwemark L. 2012. Recommendations for using XRF core scanning as a tool in tephrochronology. *The Holocene 22*, 371–375.

Lisiecki L.E. & Raymo M.E. 2005. A Pliocene–Pleistocene stack of 57 globally distributed benthic delta O-18 records. *Paleoceanography 20*, PA1003, doi: 10.1029/2004PA001071.

Löwemark L., Chen H.-F., Yang T.-N., Kylander M., Yu E.-F., Hsu Y.-W., Lee T.-Q., Song S.-R. & Jarvis S. 2011. Normalizing XRF-scanner data: a cautionary note on the interpretation of high-resolution records from organic-rich lakes. *Journal of Asian Earth Sciences 40*, 1250–1256.

Löwemark L., Jakobsson M., Mörth M. & Backman J. 2008. Arctic Ocean manganese contents and sediment colour cycles. *Polar Research 27*, 105–113.

Löwemark L., O'Regan M., Hanebuth T. & Jakobsson M. 2012. Late Quaternary spatial and temporal variability in Arctic deep-sea bioturbation and its relation to Mn cycles. *Palaeogeography Palaeoclimatology Palaeoecology 365–366*, 192–208.

Macdonald R. & Gobeil C. 2012. Manganese sources and sinks in the Arctic Ocean with reference to periodic enrichments in basin sediments. *Aquatic Geochemistry 18*, 565–591.

März C., Stratmann A., Matthiessen J., Meinhardt A.K., Eckert S., Schnetger B., Vogt C., Stein R. & Brumsack H.J. 2011. Manganese-rich brown layers in Arctic Ocean

sediments: composition, formation mechanisms, and diagenetic overprint. *Geochimica et Cosmochimica Acta 75*, 7668–7687.

Nørgaard-Pedersen N., Spielhagen R.F., Thiede J. & Kassens H. 1998. Central Arctic surface ocean environment during the past 80,000 years. *Paleoceanography 13*, 193–204.

O'Regan M., King J., Backman J., Jakobsson M., Palike H., Moran K., Heil C., Sakamoto T., Cronin T.M. & Jordan R.W. 2008. Constraints on the Pleistocene chronology of sediments from the Lomonosov Ridge. *Paleoceanography 23*, PA1S19, doi: 10.1029/2007PA001551.

Phillips R.L. & Grantz A. 2001. Regional variations in provenance and abundance of ice-rafted clasts in Arctic Ocean sediments: implications for the configuration of late Quaternary oceanic and atmospheric circulation in the Arctic. *Marine Geology 172*, 91–115.

Polyak L., Bischof J., Ortiz J.D., Darby D.A., Channell J.E.T., Xuan C., Kaufman D.S., Lovlie R., Schneider D.A., Eberl D.D., Adler R.E. & Council E.A. 2009. Late Quaternary stratigraphy and sedimentation patterns in the western Arctic Ocean. *Global and Planetary Change 68*, 5–17.

Polyak L., Curry W.B., Darby D.A., Bischof J. & Cronin T.M. 2004. Contrasting glacial/interglacial regimes in the western Arctic Ocean as exemplified by a sedimentary record from the Mendeleev Ridge. *Palaeogeography Palaeoclimatology Palaeoecology 203*, 73–93.

Sellén E., O'Regan M. & Jakobsson M. 2010. Spatial and temporal Arctic Ocean depositional regimes: a key to the evolution of ice drift and current patterns. *Quaternary Science Reviews 26*, 3644–3664.

Spielhagen R.F., Baumann K.H., Erlenkeuser H., Nowaczyk N.R., Norgaard-Pedersen N., Vogt C. & Weiel D. 2004. Arctic Ocean deep-sea record of northern Eurasian ice sheet history. *Quaternary Science Reviews 23*, 1455–1483.

Stangeew E. 2001. *Distribution and isotopic composition of living planktonic foraminifera N. pachyderma (sinistral) and T. quinqueloba in the high latitude North Atlantic*. PhD thesis, Christian Albrechts University, Kiel.

Stein R., Grobe H. & Wahsner M. 1994. Organic carbon, carbonate, and clay mineral distributions in eastern central Arctic Ocean surface sediments. *Marine Geology 119*, 269–285.

Tjallingii R., Rohl U., Kolling M. & Bickert T. 2007. Influence of the water content on x-ray fluorescence core-scanning measurements in soft marine sediments. *Geochemistry Geophysics Geosystems 8*, Q02004, doi: 10.1029/2006GC001393.

Vogt C. 1997. *Zeitliche und räumliche Verteilung von Mineralvergesellschaftungen in spätquatären Sedimenten des Arktischen Ozeans und ihre Nützlichkeit als Klimaindikatoren während der Glazial/Interglazial-Wechsel (Regional and temporal variations of mineral assemblages in Arctic Ocean sediments as climatic indicator during glacial/interglacial changes). Reports on Polar Research 251*. Bremerhaven: Alfred Wegener Institute for Polar and Marine Research.

Weltje G.J. & Tjallingii R. 2008. Calibration of XRF core scanners for quantitative geochemical logging of sediment cores: theory and application. *Earth and Planetary Science Letters 274*, 423–438.



Citation: *Polar Research* 2013, *32*, 18386, http://dx.doi.org/10.3402/polar.v32i0.18386